Supporting Information

Amphiphilic Diblock Copolymers of Poly(glycidol) with Biodegradable Polyester/Polycarbonate. Organocatalytic One-Pot ROP and Self-Assembling Property

Tingyu He,[a] Atsushi Narumi,[b] Yanqiu Wang,[a] Liang Xu,[a] Shin-ichiro Sato,[c] Xiande Shen*,[a,d] and Toyoji Kakuchi*,[a,c,d]

[a] *Research Center for Polymer Materials, School of Materials Science and Engineering, Changchun University of Science and Technology, Weixing Road 7989, Jilin 130022, China*
[b] *Graduate School of Organic Materials Science, Yamagata University, 4-3-16 Jonan, Yonezawa, Yamagata 992-8510, Japan*
[c] *Division of Applied Chemistry, Faculty of Engineering, Hokkaido University, Sapporo, Hokkaido 060-8628, Japan*
[d] *Chongqing Research Institute, Changchun University of Science and Technology, No. 618 Liangjiang Avenue, Longxing Town, Yubei District, Chongqing City 401135, China*

Contents

1. Tables for the synthesis and characterizations of PBnGE$_x$-*b*-PLAA$_y$, PBnGE$_x$-*b*-PTMC$_y$ and PBnGE$_x$-*b*-PCL$_y$

Table S1. The 1st ROP of BnGE using *t*-Bu-P$_4$ and 2nd ROP of LLA using *t*-Bu-P$_2$ to produce PBnGE$_x$-*b*-PLLA$_y$

Entry	1st ROP of BnGE [a]			2nd ROP of LLA [b]			Product			
	$[M_{1st}]_0/[I]_0$	Time (h)	Conv. (%)	$[M_{2nd}]_0/[I]_0$	Time (h)	Conv. (%)	Code[c]	$M_{n,calcd}$ [d] (kg mol^{-1})	$M_{n,NMR}$ [e] (kg mol^{-1})	$Đ$ [f]
1	50	20	>99	50	6	>99	PBnGE$_{49}$-*b*-PLLA$_{49}$	15.6	15.3	1.11
2	50	20	>99	75	6	>99	PBnGE$_{49}$-*b*-PLLA$_{73}$	19.0	18.7	1.13
3	50	20	>99	100	6	98.5	PBnGE$_{49}$-*b*-PLLA$_{92}$	22.6	21.5	1.15
4	50	20	>99	125	6	94.8	PBnGE$_{49}$-*b*-PLLA$_{115}$	25.5	24.8	1.16
5	50	20	>99	150	6	90.6	PBnGE$_{49}$-*b*-PLLA$_{132}$	28.0	27.2	1.17
6	75	20	>99	50	6	>99	PBnGE$_{73}$-*b*-PLLA$_{49}$	19.7	19.2	1.14
7	100	20	>99	50	6	>99	PBnGE$_{98}$-*b*-PLLA$_{49}$	23.8	23.3	1.15
8	125	24	95.2	50	6	>99	PBnGE$_{115}$-*b*-PLLA$_{49}$	26.9	26.1	1.16
9	150	28	92.1	50	6	>99	PBnGE$_{132}$-*b*-PLLA$_{49}$	30.2	28.9	1.17

[a] The polymerizations of BnGE (M_{1st}) were performed using *t*BBA as the initiator (I) and *t*-Bu-P$_4$ as the catalyst (Cat_{1st}) in THF at room temperature ($[M_{1st}]_0$, 3 mol L^{-1}; $[I]/[Cat_{1st}]$, 1/0.5). [b] The polymerizations of LLA (M_{2nd}) were performed using *t*-Bu-P$_2$ as the catalyst (Cat_{2nd}) after the "organocatalyst switching" procedure using the $[Cat_{1st}]_0/[DPP]_0/[Cat_{2nd}]_0$ ratio of 1:1.3:2.3. [c] The number average degree of polymerizations of the PBnGE and PLLA units (*x* and *y*, respectively) were determined by ^{1}H NMR spectra in $CDCl_3$. [d] Calculated from the equation: $M_{n,calcd}$ = {($[M_{1st}]_0/[I]_0$) × (conv. for the 1st ROP) × (MW of M_{1st})} + {($[M_{2nd}]_0/[I]_0$) × (conv. for the 2nd ROP) × (MW of M_{2nd})]} + {(MW of I)}. [e] Determined by ^{1}H NMR spectra in $CDCl_3$. [f] Determined by SEC in THF using PS standards.

Table S2. The 1st ROP of BnGE using *t*-Bu-P_4 and 2nd ROP of TMC using *t*-Bu-P_2 to produce PBnGE$_x$-*b*-PTMC$_y$

Entry	1st ROP of BnGE [a]			2nd ROP of TMC [b]			Product			
	$[M_{1st}]_0/[I]_0$	Time (h)	Conv. (%)	$[M_{2nd}]_0/[I]_0$	Time (h)	Conv. (%)	Code [c]	$M_{n,calcd}$ [d] (kg mol^{-1})	$M_{n,NMR}$ [e] (kg mol^{-1})	$Đ$ [f]
10	50	20	>99	50	6	>99	PBnGE$_{49}$-*b*-PTMC$_{49}$	13.5	13.1	1.09
11	50	20	>99	75	6	>99	PBnGE$_{49}$-*b*-PTMC $_{73}$	16.0	15.7	1.12
12	50	20	>99	100	6	96.6	PBnGE$_{49}$-*b*-PTMC$_{95}$	18.2	17.9	1.15
13	50	20	>99	125	6	92.8	PBnGE$_{49}$-*b*- PTMC$_{114}$	20.2	19.9	1.17
14	50	20	>99	150	6	89.4	PBnGE$_{49}$-*b*- PTMC$_{130}$	22.1	21.5	1.18
15	75	20	>99	50	6	>99	PBnGE$_{74}$-*b*- PTMC$_{49}$	17.6	17.3	1.12
16	100	20	>99	50	6	>99	PBnGE$_{98}$-*b*- PTMC $_{49}$	21.7	21.3	1.13
17	125	24	94.8	50	6	>99	PBnGE$_{114}$-*b*- PTMC$_{48}$	24.7	23.8	1.14
18	150	28	91.1	50	6	>99	PBnGE$_{133}$-*b*- PTMC$_{48}$	27.7	26.9	1.15

[a] The polymerizations of BnGE (M_{1st}) were performed using *t*BBA as the initiator (I) and *t*-Bu-P_4 as the catalyst (Cat_{1st}) in THF at room temperature ($[M_{1st}]_0$, 3 mol L^{-1}; $[I]/[Cat_{1st}]$, 1/0.5). [b] The polymerizations of TMC (M_{2nd}) were performed using *t*-Bu-P_2 as the catalyst (Cat_{2nd}) after the "organocatalyst switching" procedure using the $[Cat_{1st}]_0/[DPP]_0/[Cat_{2nd}]_0$ ratio of 1:1.3:2.3. [c] The number average degree of polymerizations of the PBnGE and PTMC units (*x* and *y*, respectively) were determined by ^{1}H NMR spectra in $CDCl_3$. [d] Calculated from the equation: $M_{n,calcd} = \{([M_{1st}]_0/[I]_0) \times (\text{conv. for the 1st ROP}) \times (\text{MW of } M_{1st})\} + \{([M_{2nd}]_0/[I]_0) \times (\text{conv. for the 2nd ROP}) \times (\text{MW of } M_{2nd})]\} + \{(\text{MW of I})\}$. [e] Determined by ^{1}H NMR spectra in $CDCl_3$. [f] Determined by SEC in THF using PS standards.

Table S3. The 1st ROP of BnGE using *t*-Bu-P_4 and 2nd ROP of LLA using *t*-Bu-P_2 to produce PBnGE$_x$-*b*-PCL$_y$

Entry	1st ROP of BnGE [a]			2nd ROP of CL [b]			Product			
	$[M_{1st}]_0/[I]_0$	Time (h)	Conv. (%)	$[M_{2nd}]_0/[I]_0$	Time (h)	Conv. (%)	Code [c]	$M_{n,calcd}$ [d] (kg mol^{-1})	$M_{n,NMR}$ [e] (kg mol^{-1})	$Đ$ [f]
19	50	20	>99	50	6	>99	PBnGE$_{49}$-*b*-PCL$_{48}$	14.1	13.7	1.08
20	50	20	>99	75	6	>99	PBnGE$_{49}$-*b*-PCL$_{72}$	16.9	16.4	1.10
21	50	20	>99	100	6	88.5	PBnGE$_{49}$-*b*-PCL$_{86}$	18.5	18.0	1.15
22	50	20	>99	125	6	84.4	PBnGE$_{49}$-*b*-PCL$_{103}$	20.4	20.0	1.18
23	50	20	>99	150	6	80.7	PBnGE$_{49}$-*b*-PCL$_{120}$	22.4	22.0	1.19
24	75	20	>99	50	6	>99	PBnGE$_{72}$-*b*-PCL$_{48}$	18.9	17.5	1.10
25	100	20	>99	50	6	>99	PBnGE$_{97}$-*b*-PCL$_{48}$	22.3	21.6	1.12
26	125	24	96.4	50	6	>99	PBnGE$_{118}$-*b*-PCL$_{48}$	25.7	25.0	1.16
27	150	28	93.3	50	6	>99	PBnGE$_{136}$-*b*-PCL$_{48}$	28.6	28.0	1.18

[a] The polymerizations of BnGE (M_{1st}) were performed using *t*BBA as the initiator (I) and *t*-Bu-P_4 as the catalyst (Cat_{1st}) in THF at room temperature ($[M_{1st}]_0$, 3 mol L^{-1}; $[I]/[Cat_{1st}]$, 1/0.5). [b] The polymerizations of CL (M_{2nd}) were performed using *t*-Bu-P_2 as the catalyst (Cat_{2nd}) after the "organocatalyst switching" procedure using the $[Cat_{1st}]_0/[DPP]_0/[Cat_{2nd}]_0$ ratio of 1:1.3:2.3. [c] The number average degree of polymerizations of the PBnGE and PCL units (*x* and *y*, respectively) were determined by ^{1}H NMR spectra in $CDCl_3$. [d] Calculated from the equation: $M_{n,calcd}$ = {($[M_{1st}]_0/[I]_0$) × (conv. for the 1st ROP) × (MW of M_{1st})} + {($[M_{2nd}]_0/[I]_0$) × (conv. for the 2nd ROP) × (MW of M_{2nd})]} + {(MW of I)}. [e] Determined by ^{1}H NMR spectra in $CDCl_3$. [f] Determined by SEC in THF using PS standards.

2. SEC traces of PBnGE$_x$-*b*-PLLA$_y$, PBnGE$_x$-*b*-PTMC$_y$ and PBnGE$_x$-*b*-PCL$_y$

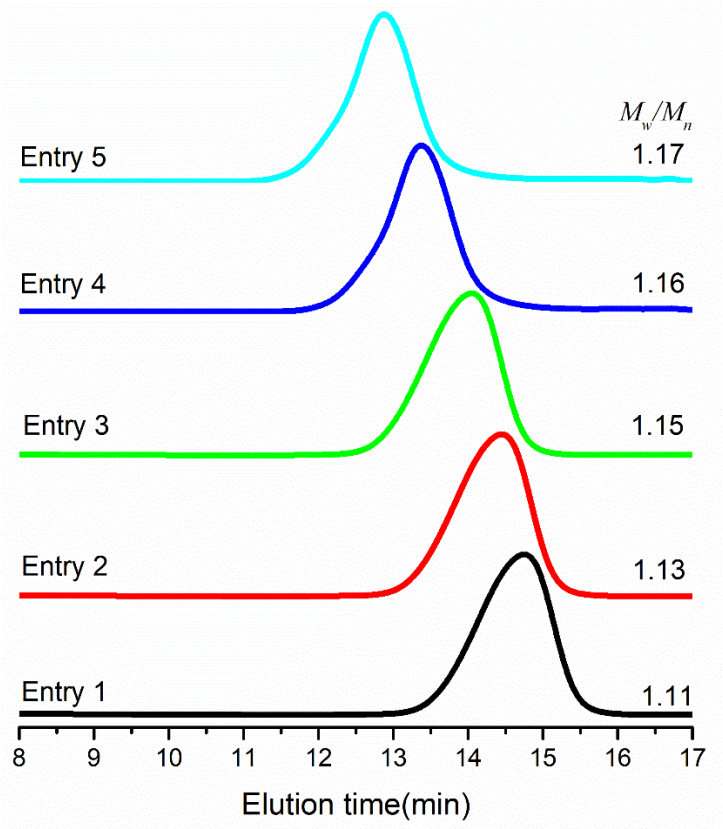

Fig. S1. SEC traces of PBnGE$_x$-*b*-PLLA$_y$ using THF as the eluent with the flow rate of 1 mL min^{-1} Entries 1, 2, 3, 4, and 5 in Table S1).

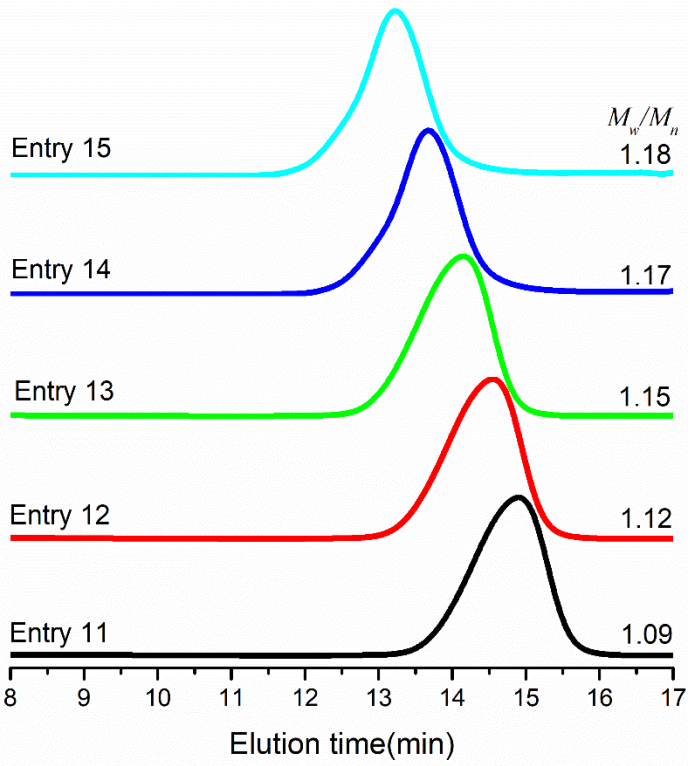

Fig. S2. SEC traces of PBnGE$_x$-*b*-PTMC$_y$ using THF as the eluent with the flow rate of 1 mL min^{-1} (Entries 10, 11, 12, 13, and 15 in Table S2).

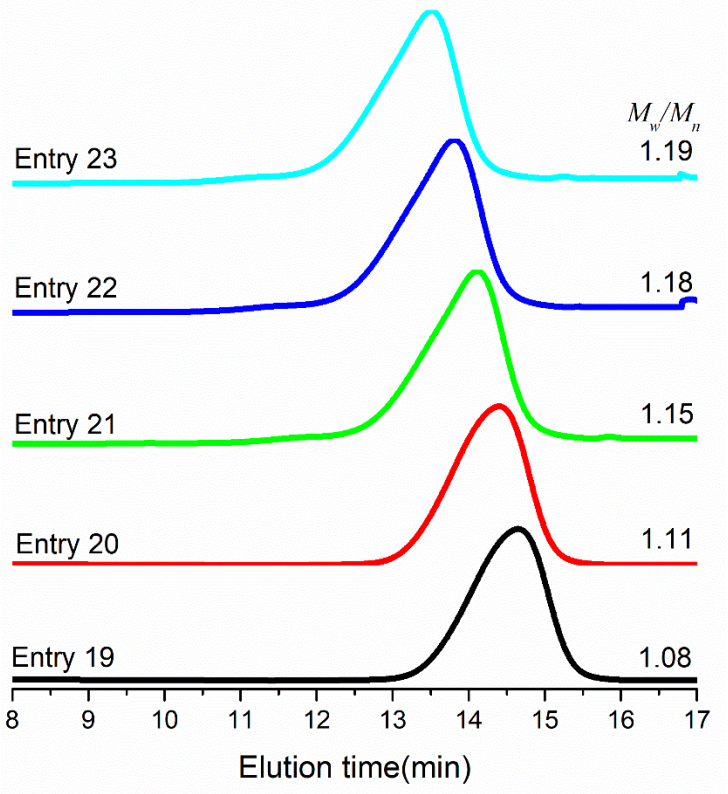

Fig. S3. SEC traces of PBnGE$_x$-*b*-PCL$_y$ using THF as the eluent with the flow rate of 1 mL min^{-1} (Entries 19, 20, 21, 22, and 23 in Table S3).

3. ^{1}H and ^{13}C NMR spectra of PBnGE$_x$-*b*-PLLA$_y$, PBnGE$_x$-*b*-PTMC$_y$ and PBnGE$_x$-*b*-PCL$_y$

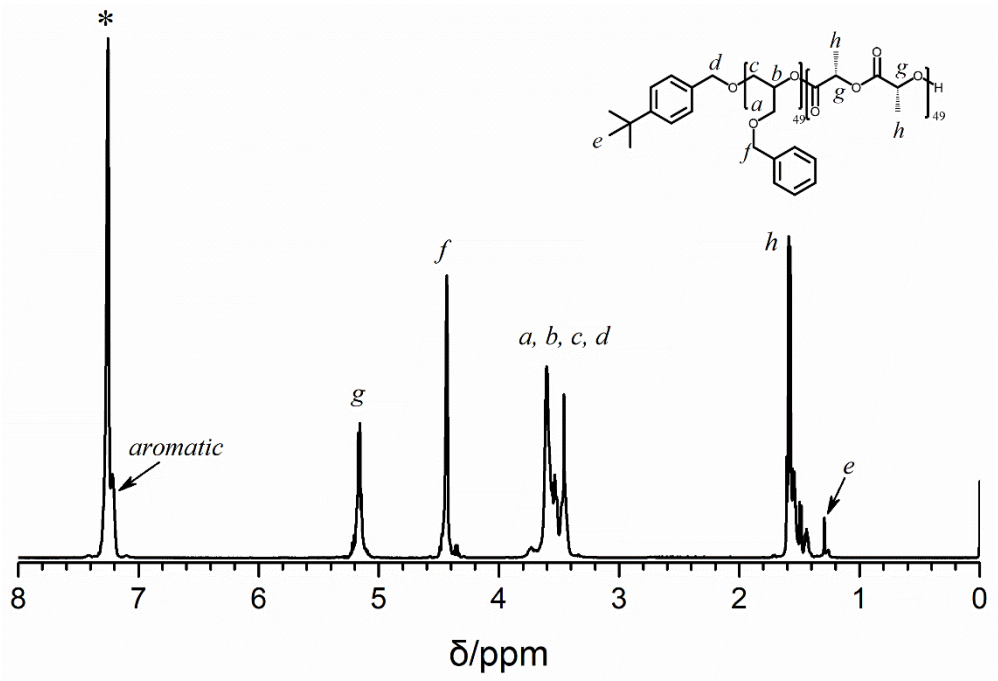

Fig. S4. The ^{1}H NMR spectrum of PBnGE$_{49}$-*b*-PLLA$_{49}$ in $CDCl_3$ (the symbol * refers to solvent peaks).

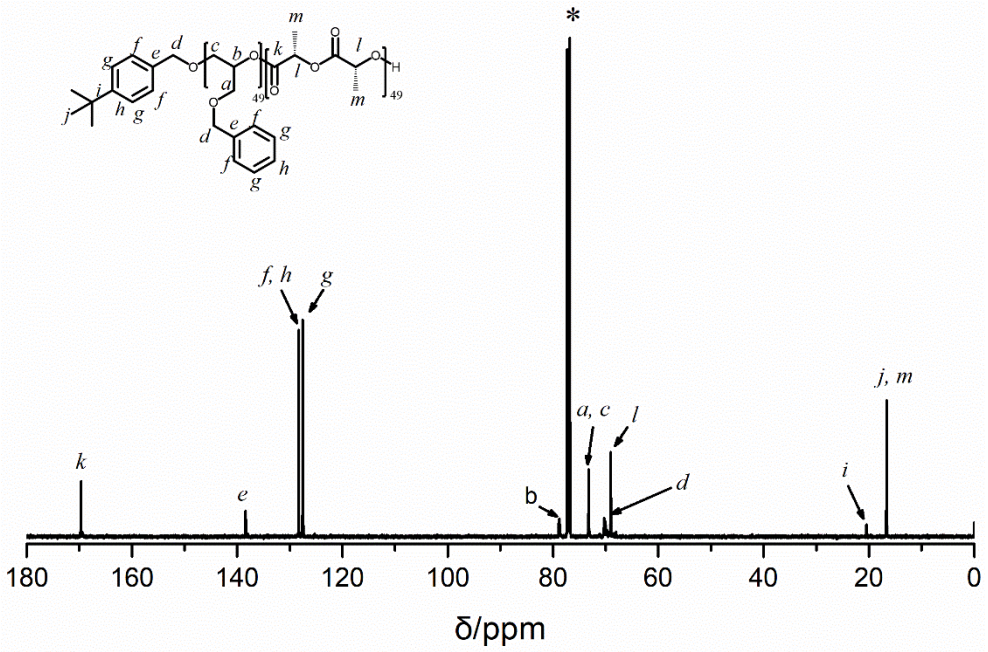

Fig. S5. The ^{13}C NMR spectrum of PBnGE$_{49}$-*b*-PLLA$_{49}$ in $CDCl_3$ (the symbol * refers to solvent peaks).

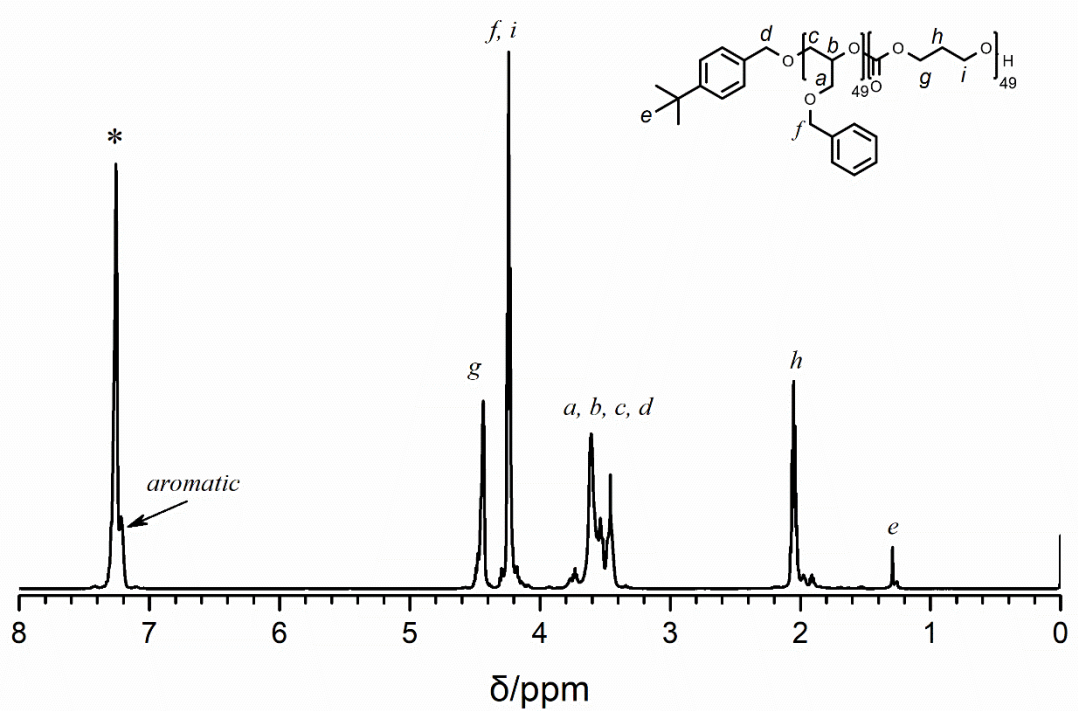

Fig. S6. ^{1}H NMR spectrum of PBnGE$_{49}$-*b*-PTMC$_{49}$ in $CDCl_3$ (the symbol * refers to solvent peaks).

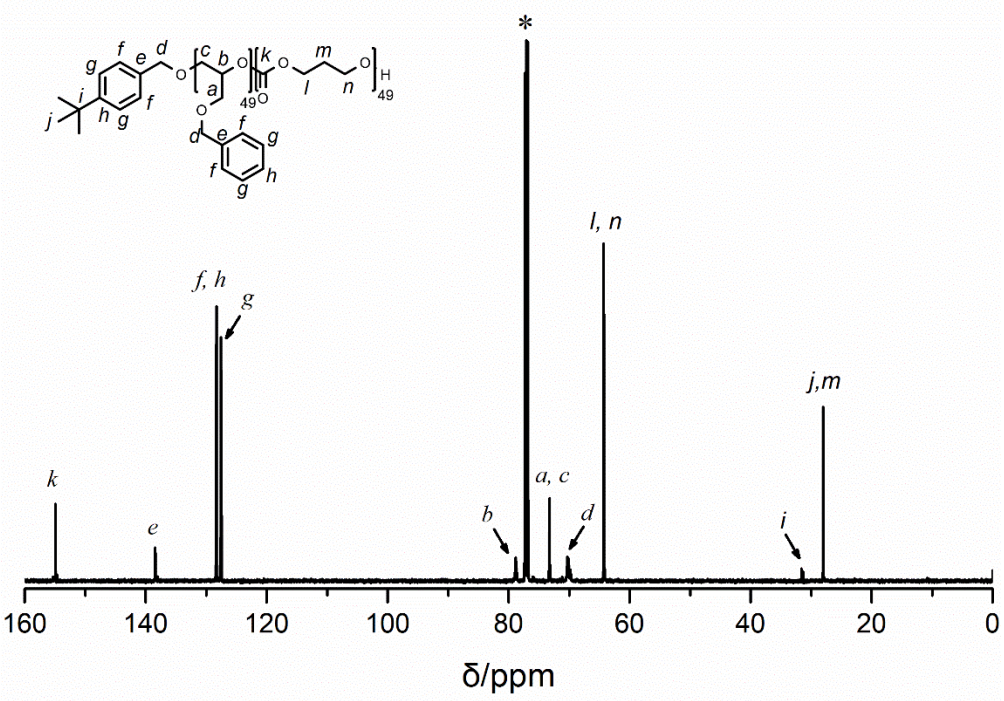

Fig. S7. ^{13}C NMR spectrum of PBnGE$_{49}$-*b*-PTMC$_{49}$ in $CDCl_3$ (the symbol * refers to solvent peaks).

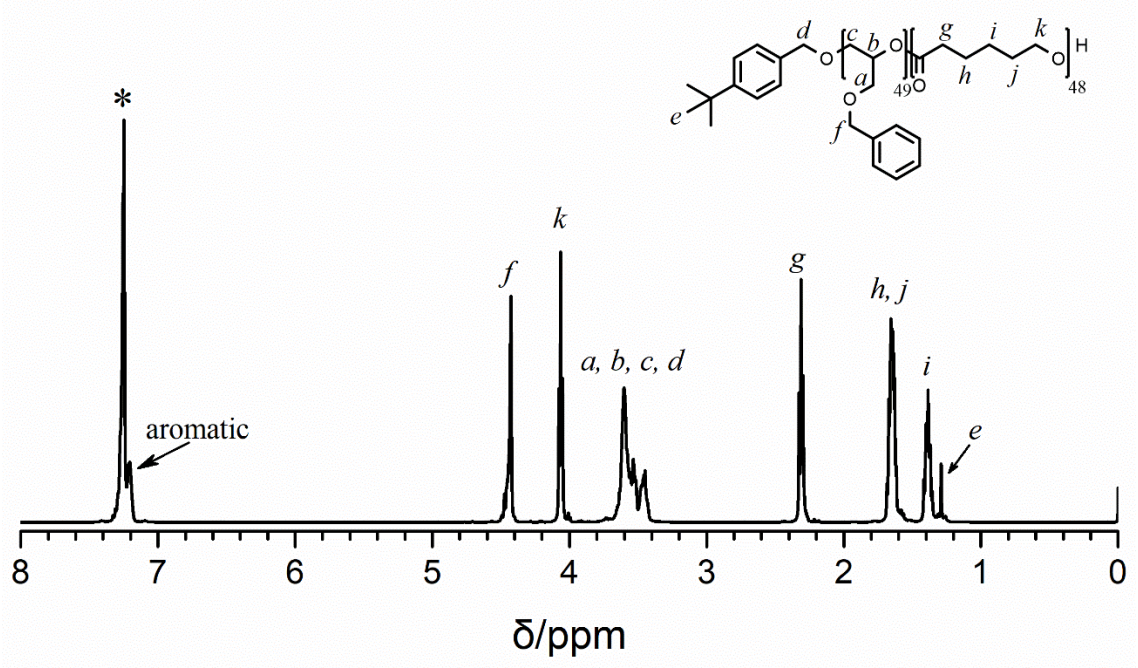

Fig. S8. ^{1}H NMR spectrum of PBnGE$_{49}$-*b*-PCL$_{49}$ in $CDCl_3$ (the symbol * refers to solvent peaks).

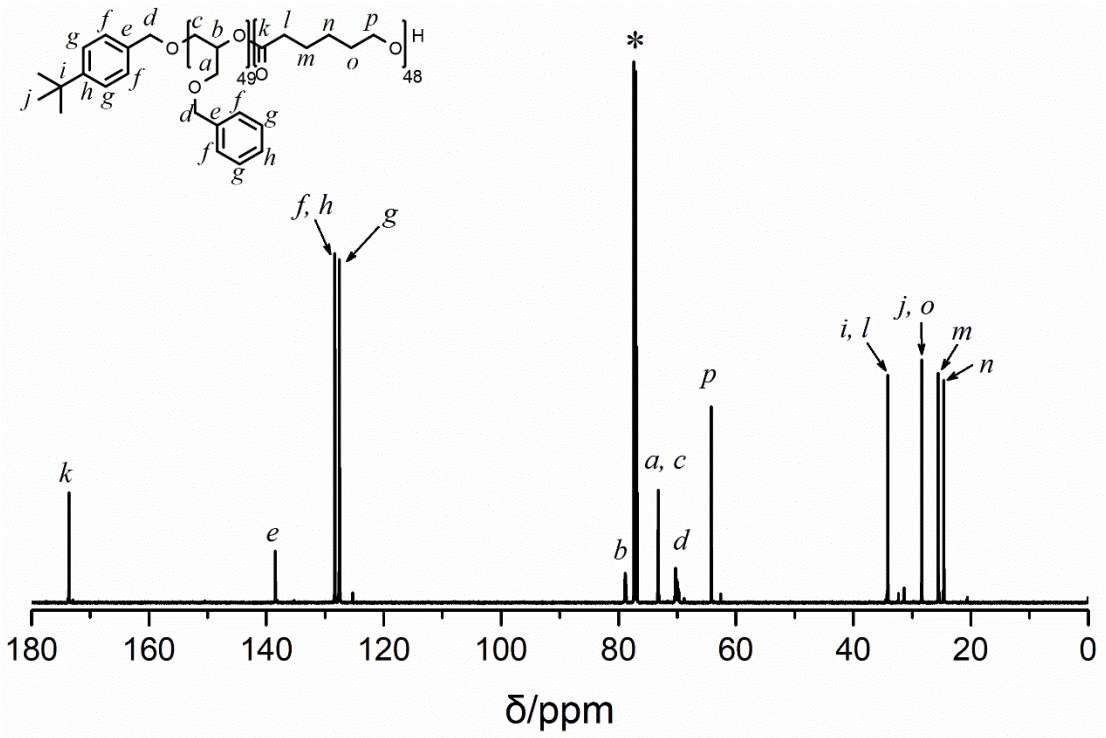

Fig. S9. ^{13}C NMR spectrum of PBnGE$_{49}$-*b*-PCL$_{49}$ in $CDCl_3$ (the symbol * refers to solvent peaks).

4. Tables for the synthesis and characterizations of PG_x-*b*-$PLLA_y$, PG_x-*b*-$PTMC_y$ and PG_x-*b*-PCL_y

Table S4. Characterizations of PG_x-*b*-$PLLA_y$ synthesized by de-benzylation of $PBnGE_x$-*b*-$PLLA_y$ [a]

Entry	Starting material	Yield (%)	Product		$Đ$ [c]	CMC × 10^3 [d] (mg mL^{-1})
			Code	$M_{w,MALS}$ [b] (kg mol^{-1})		
28	$PBnGE_{49}$-*b*-$PLLA_{49}$	88.7	PG_{48}-*b*-$PLLA_{49}$	10.6	1.13	5.72
29	$PBnGE_{49}$-*b*-$PLLA_{73}$	86.2	PG_{48}-*b*-$PLLA_{73}$	14.1	1.14	5.32
30	$PBnGE_{49}$-*b*-$PLLA_{92}$	79.8	PG_{48}-*b*-$PLLA_{92}$	16.8	1.17	4.97
31	$PBnGE_{49}$-*b*-$PLLA_{115}$	80.5	PG_{48}-*b*-$PLLA_{115}$	20.1	1.18	4.58
32	$PBnGE_{49}$-*b*-$PLLA_{132}$	75.9	PG_{48}-*b*-$PLLA_{132}$	22.6	1.19	4.22
33	$PBnGE_{73}$-*b*-$PLLA_{49}$	84.7	PG_{70}-*b*-$PLLA_{49}$	12.3	1.14	6.06
34	$PBnGE_{98}$-*b*-$PLLA_{49}$	77.8	PG_{95}-*b*-$PLLA_{49}$	14.1	1.15	6.44
35	$PBnGE_{115}$-*b*-$PLLA_{49}$	74.2	PG_{114}-*b*-$PLLA_{49}$	15.5	1.15	6.73
36	$PBnGE_{132}$-*b*-$PLLA_{49}$	75.5	PG_{130}-*b*-$PLLA_{49}$	16.7	1.16	7.10

[a] Determined by the SEC equipped with a MALS in DMF in the presence of 0.01 M LiCl. [b] Determined by MALS in DMF containing 0.01 mol L^{-1} LiCl. [c] Determined by SEC in DMF using PMMA standards. [d] Determined by fluorescence spectroscopy using pyrene as the probe.

Table S5 Characterizations of PG_x-*b*-$PTMC_y$ synthesized by de-benzylation of $PBnGE_x$-*b*-$PTMC_y$ [a]

Entry	Starting material	Yield (%)	Product		$Đ$ [c]	CMC × 10^3 [d] (mg mL^{-1})
			Code	$M_{w,MALS}$ [b] (kg mol^{-1})		
37	$PBnGE_{49}$-*b*-$PTMC_{49}$	89.6	PG_{48}-*b*-$PTMC_{49}$	8.6	1.12	3.05
38	$PBnGE_{49}$-*b*-$PTMC_{73}$	82.1	PG_{48}-*b*-$PTMC_{73}$	11.0	1.14	2.62
39	$PBnGE_{49}$-*b*-$PTMC_{95}$	80.4	PG_{48}-*b*-$PTMC_{95}$	13.3	1.17	2.39
40	$PBnGE_{49}$-*b*-$PTMC_{125}$	75.6	PG_{47}-*b*-$PTMC_{114}$	15.2	1.19	2.08
41	$PBnGE_{50}$-*b*-$PTMC_{150}$	73.8	PG_{48}-*b*-$PTMC_{130}$	16.9	1.20	1.66
42	$PBnGE_{74}$-*b*-$PTMC_{49}$	80.5	PG_{70}-*b*-$PTMC_{49}$	10.2	1.12	3.37
43	$PBnGE_{98}$-*b*-$PTMC_{49}$	82.6	PG_{94}*b*-$PTMC_{49}$	12.0	1.12	3.65
44	$PBnGE_{114}$-*b*-$PTMC_{48}$	78.3	PG_{110}-*b*-$PTMC_{48}$	13.1	1.14	3.99
45	$PBnGE_{133}$-*b*-$PTMC_{48}$	70.9	PG_{129}-*b*-$PTMC_{48}$	14.5	1.16	4.27

[a] Determined using the SEC equipped with a MALS in DMF in the presence of 0.01 M LiCl. [b] Determined by MALS in DMF containing 0.01 mol L^{-1} LiCl. [c] Determined by SEC in DMF using PMMA standards. [d] Determined by fluorescence spectroscopy using pyrene as the probe.

Table S6 Characterizations of PG_x-*b*-PCL_y synthesized by de-benzylation of $PBnGE_x$-*b*-PCL_y [a]

Entry	Starting material	Yield (%)	Product		$Đ$ [c]	CMC × 10^3 [d] (mg mL^{-1})
			Code	$M_{w,MALS}$ [b] (kg mol^{-1})		
46	$PBnGE_{49}$-*b*-PCL_{48}	86.7	PG_{47}-*b*-PCL_{48}	9.0	1.16	0.87
47	$PBnGE_{49}$-*b*-PCL_{72}	81.8	PG_{47}-*b*-PCL_{72}	11.7	1.14	0.62
48	$PBnGE_{49}$-*b*-PCL_{86}	78.2	PG_{47}-*b*-PCL_{86}	13.3	1.17	0.40
49	$PBnGE_{49}$-*b*-PCL_{103}	76.1	PG_{47}-*b*-PCL_{103}	15.3	1.19	0.22
50	$PBnGE_{49}$-*b*-PCL_{120}	72.9	PG_{47}-*b*-PCL_{120}	17.2	1.21	0.14
51	$PBnGE_{72}$-*b*-PCL_{48}	80.7	PG_{70}-*b*-PCL_{48}	10.7	1.17	0.93
52	$PBnGE_{97}$-*b*-PCL_{48}	78.4	PG_{93}-*b*-PCL_{48}	12.4	1.13	1.08
53	$PBnGE_{118}$-*b*-PCL_{48}	79.5	PG_{112}-*b*-PCL_{48}	13.8	1.14	1.35
54	$PBnGE_{136}$-*b*-PCL_{48}	74.4	PG_{130}-*b*-PCL_{48}	15.1	1.18	1.58

[a] Determined by the SEC equipped with a MALS in DMF in the presence of 0.01 M LiCl. [b] Determined by MALS in DMF containing 0.01 mol L^{-1} LiCl. [c] Determined by SEC in DMF using PMMA standards. [d] Determined by fluorescence spectroscopy using pyrene as the probe.

5. SEC traces of PG_x-*b*-$PLLA_y$, PG_x-*b*-$PTMC_y$ and PG_x-*b*-PCL_y

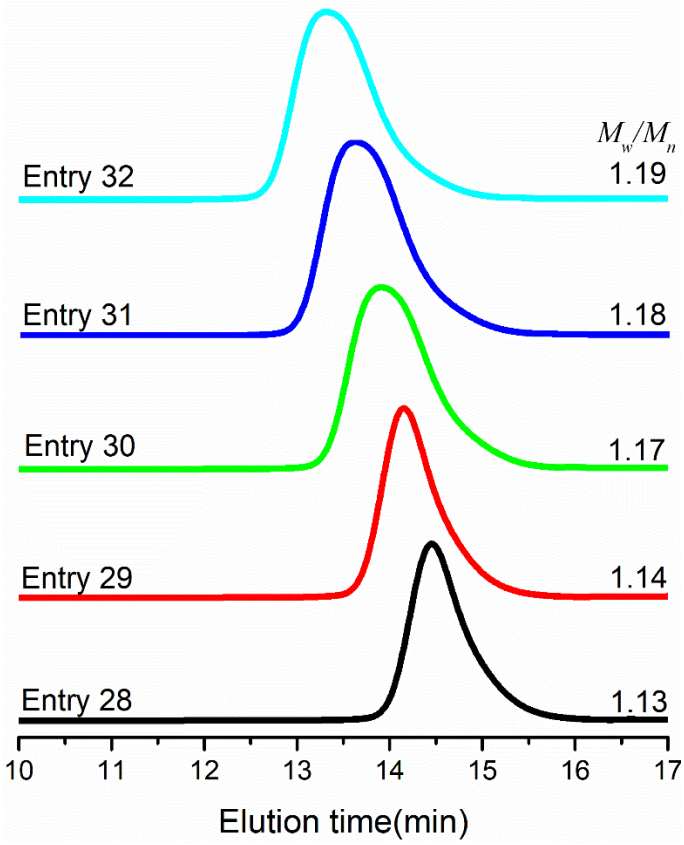

Fig. S10. SEC traces of PG_x-*b*-$PLLA_y$ using DMF as the eluent with the flow rate of 1 mL min^{-1} (Entries 28, 29, 30, 31, and 32 in Table S4).

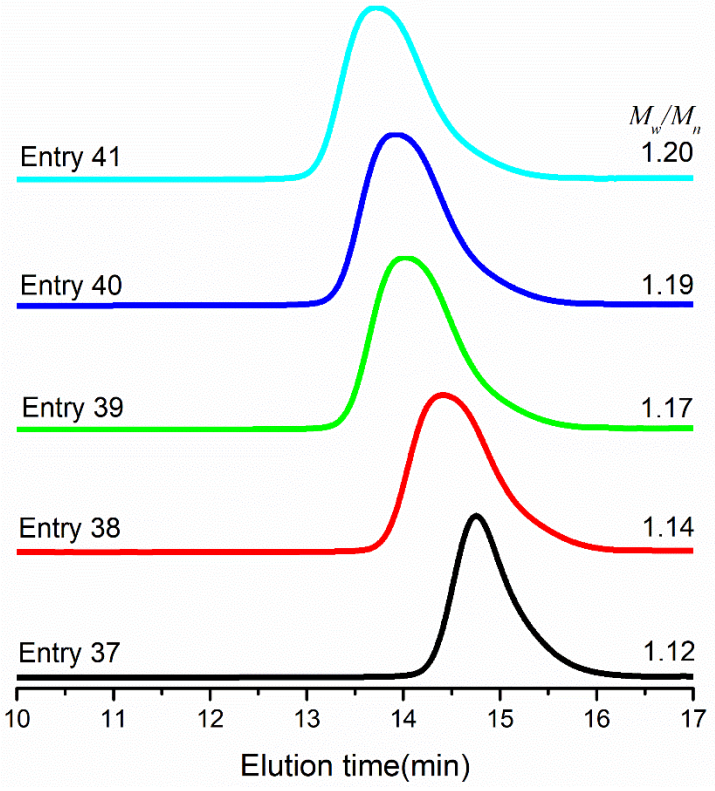

Fig. S11. SEC traces of PG_x-*b*-$PTMC_y$ using DMF as the eluent with the flow rate of 1 mL min^{-1} (Entries 37, 38, 39, 40, and 41 in Table S5).

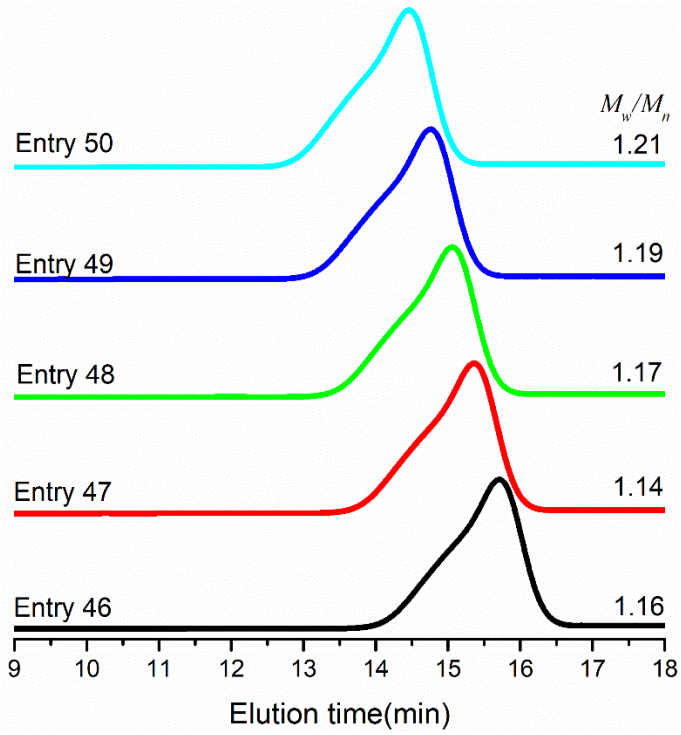

Fig. S12. SEC traces of PG_x-*b*-PCL_y using DMF as the eluent with the flow rate of 1 mL min^{-1} (Entries 46, 47, 48, 49, and 50 in Table S6).

6. ^{1}H and ^{13}C NMR spectra of PG_{48}-*b*-$PLLA_{49}$, PG_{49}-*b*-$PTMC_{49}$ and PG_{49}-*b*-PCL_{49}

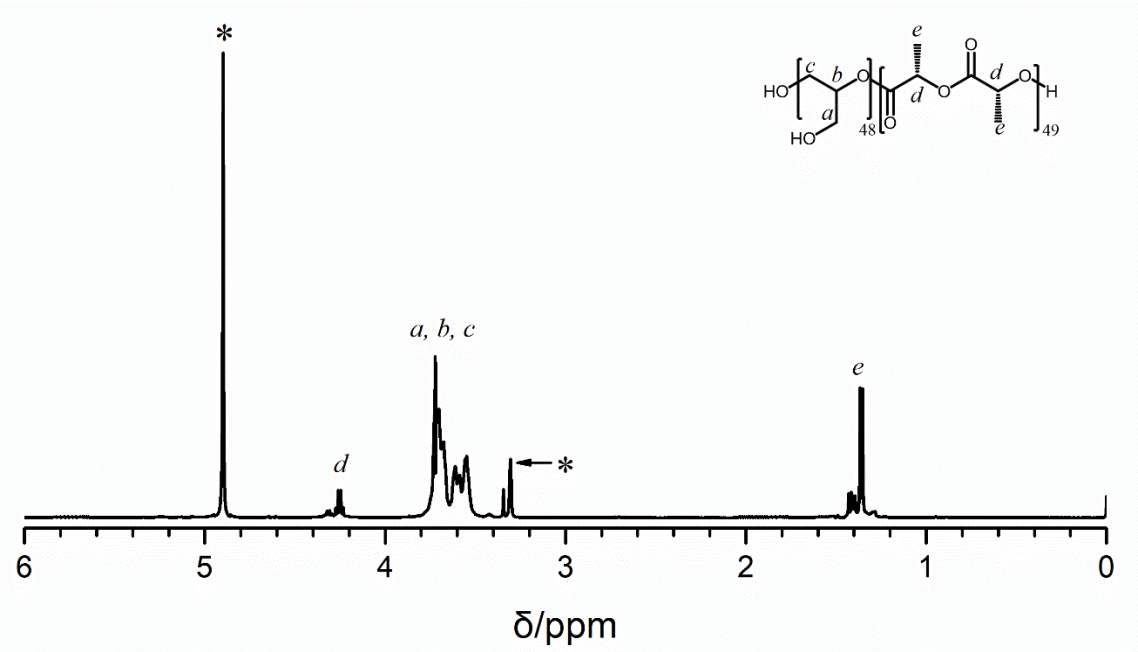

Fig. S13. The ^{1}H NMR spectrum of PG_{48}-*b*-$PLLA_{49}$ in CD_3OD (the symbol * refers to solvent peaks).

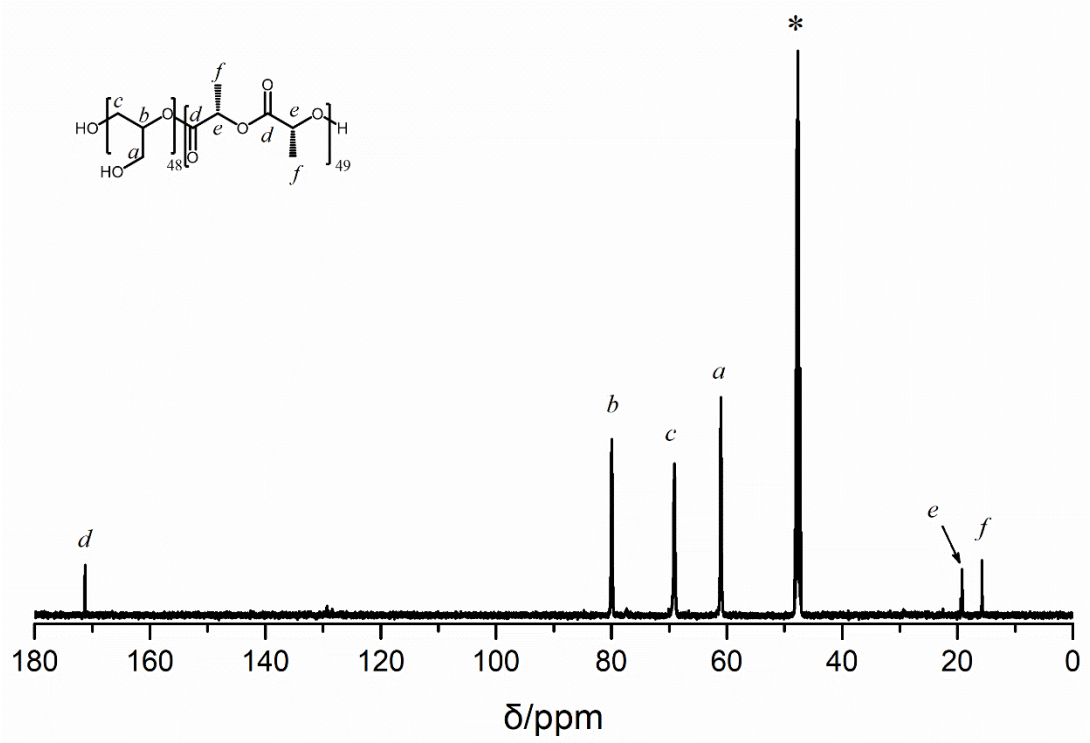

Fig. S14. The ^{13}C NMR spectrum of PG_{48}-*b*-$PLLA_{49}$ in CD_3OD (the symbol * refers to solvent peaks).

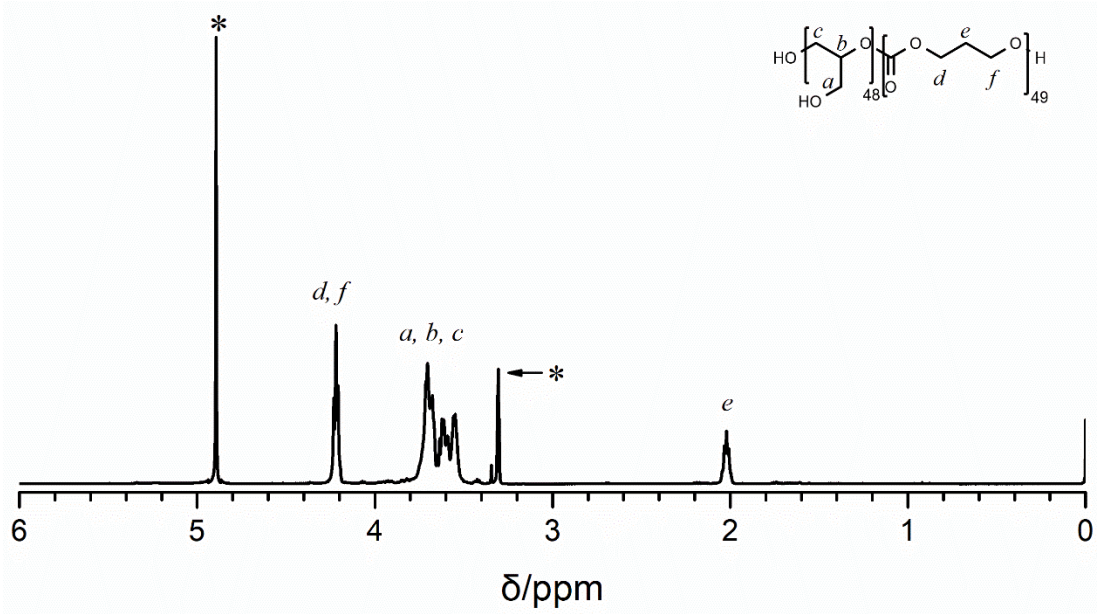

Fig. S15. ^{1}H NMR spectrum of PG_{49}-*b*-$PTMC_{49}$ in CD_3OD (the symbol * refers to solvent peaks).

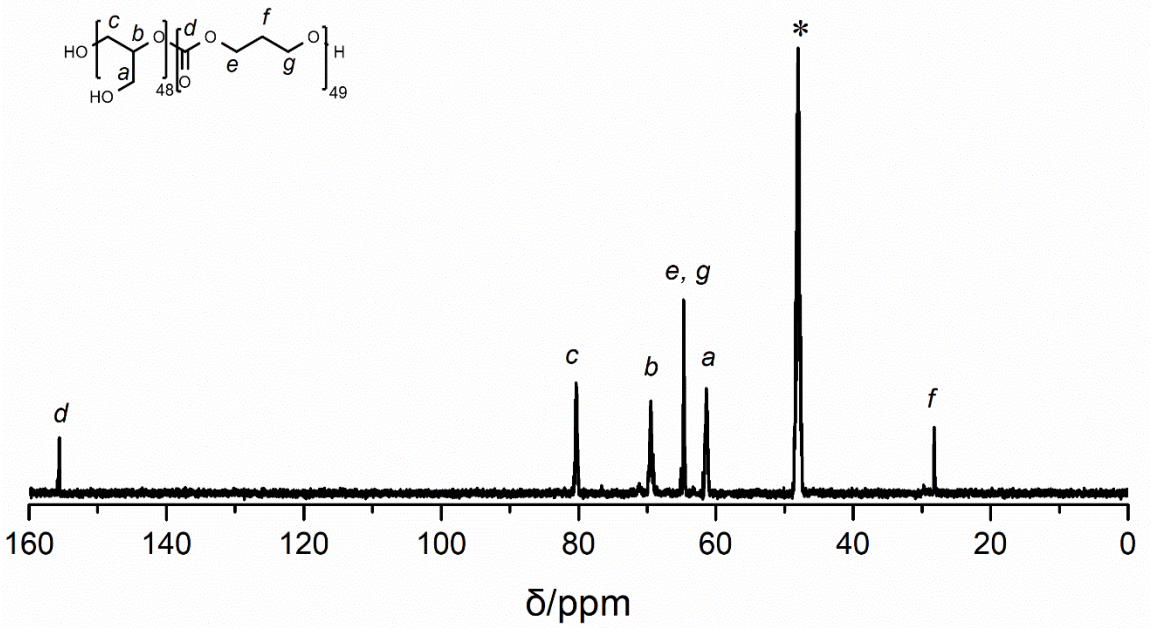

Fig. S16. ^{13}C NMR spectrum of PG_{49}-*b*-$PTMC_{49}$ in CD_3OD (the symbol * refers to solvent peaks).

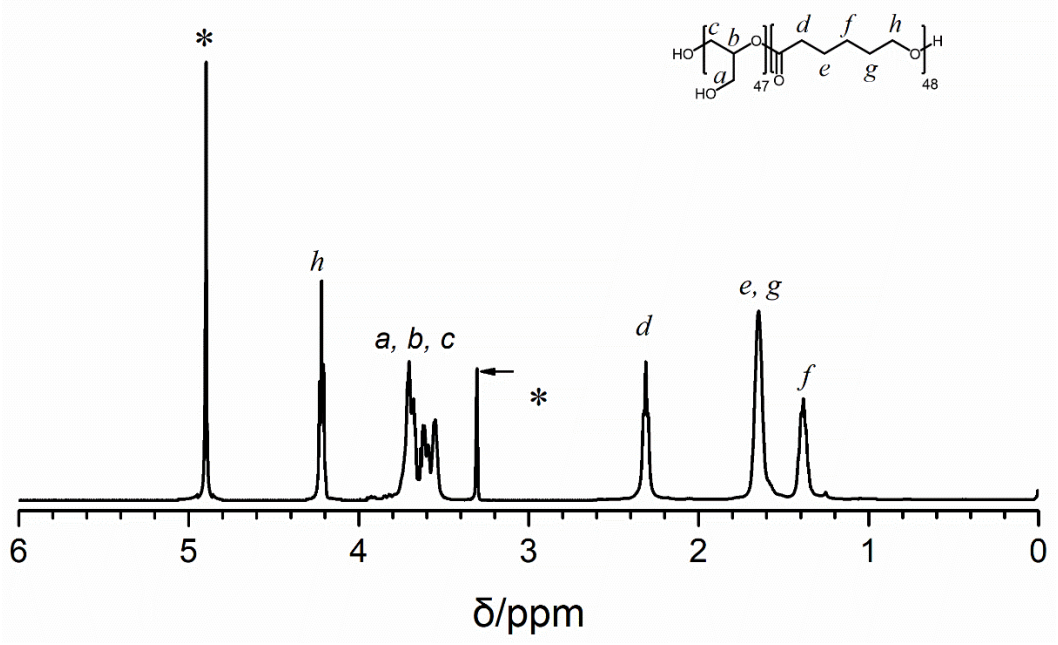

Fig. S17. ^{1}H NMR spectrum of PG_{49}-*b*-PCL_{49} in CD_3OD (the symbol * refers to solvent peaks).

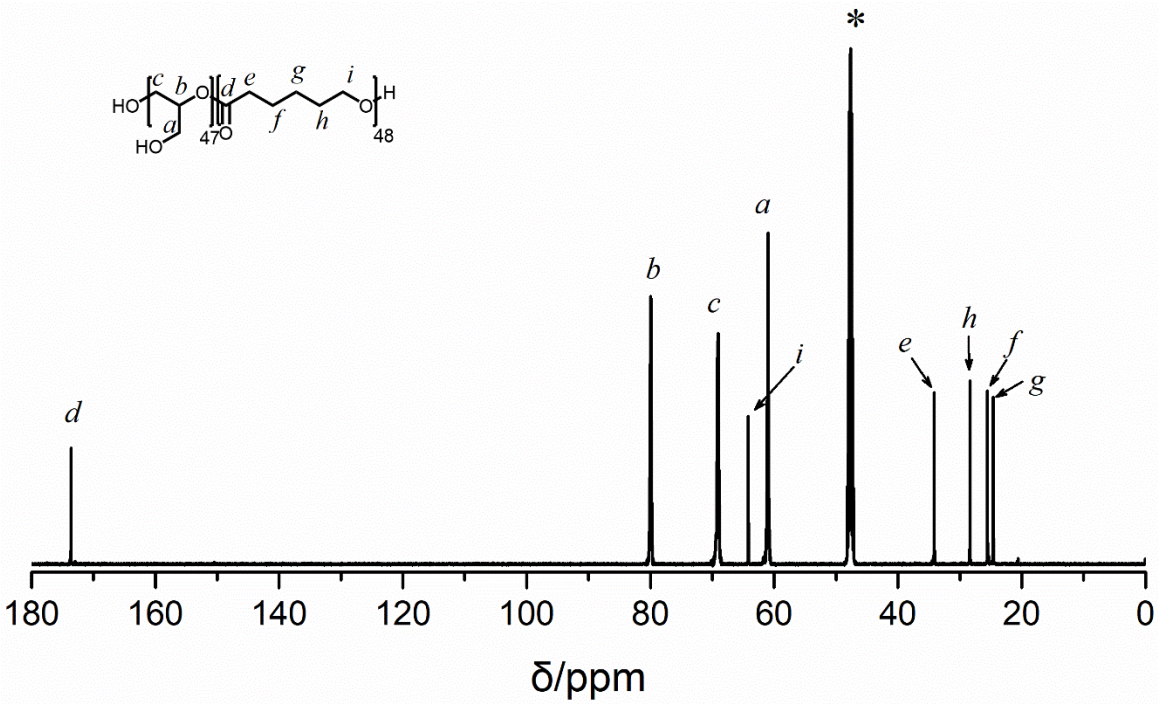

Fig. S18. ^{13}C NMR spectrum of PG_{49}-*b*-PCL_{49} in CD_3OD (the symbol * refers to solvent peaks).

7. Table for the hydrodynamic diameters (D_hs) of PG$_x$-*b*-PLLA$_y$, PG$_x$-*b*-PTMC$_y$ and PG$_x$-*b*-PCL$_y$

Table S7. The hydrodynamic diameters (D_hs) of PG$_x$-*b*-PLLA$_y$, PG$_x$-*b*-PTMC$_y$ and PG$_x$-*b*-PCL$_y$

Code	D_h (nm)	Code	D_h (nm)	Code	D_h (nm)
PG$_{48}$-*b*-PLLA$_{49}$	56	PG$_{48}$-*b*-PTMC$_{49}$	62	PG$_{47}$-*b*-PCL$_{48}$	80
PG$_{48}$-*b*-PLLA$_{73}$	60	PG$_{48}$-*b*-PTMC$_{73}$	66	PG$_{47}$-*b*-PCL$_{72}$	84
PG$_{48}$-*b*-PLLA$_{92}$	66	PG$_{48}$-*b*-PTMC$_{95}$	71	PG$_{47}$-*b*-PCL$_{86}$	88
PG$_{48}$-*b*-PLLA$_{115}$	74	PG$_{47}$-*b*-PTMC$_{114}$	77	PG$_{47}$-*b*-PCL$_{103}$	92
PG$_{48}$-*b*-PLLA$_{132}$	80	PG$_{48}$-*b*-PTMC$_{130}$	84	PG$_{47}$-*b*-PCL$_{120}$	96
PG$_{70}$-*b*-PLLA$_{49}$	75	PG$_{70}$-*b*-PTMC$_{49}$	80	PG$_{70}$-*b*-PCL$_{48}$	87
PG$_{95}$-*b*-PLLA$_{49}$	79	PG$_{94}$*b*-PTMC$_{49}$	83	PG$_{93}$-*b*-PCL$_{48}$	90
PG$_{114}$-*b*-PLLA$_{49}$	83	PG$_{110}$-*b*-PTMC$_{48}$	87	PG$_{112}$-*b*-PCL$_{48}$	94
PG$_{130}$-*b*-PLLA$_{49}$	89	PG$_{129}$-*b*-PTMC$_{48}$	91	PG$_{130}$-*b*-PCL$_{48}$	98